Progress In Electromagnetics Research, PIER 74, 353–377, 2007

AN EFFICIENT ANALYSIS OF VERTICAL DIPOLE ANTENNAS ABOVE A LOSSY HALF-SPACE

X.-B. Xu and Y. F. Huang

Holcombe Department of Electrical & Computer Engineering
Clemson University
Clemson, SC 29634-0915, USA

Abstract—The electromagnetic modeling of radiation by vertical dipole antennas above a lossy half-space is an important subject. The modeling often encounters Sommerfeld-type integrals that are normally highly oscillatory with poor convergence. Recently, an efficient computation of the electric field radiated by an infinitesimal electric dipole above a lossy half-space has been reported, in which the Sommerfeld-type integrals are reduced to rapidly-converging integrals. Using such efficiently-calculated electric field as the Green's function, in this paper, an electric field integral equation (EFIE) is formulated for the analysis of a vertical dipole antenna above a lossy half-space. Then, the EFIE is solved numerically employing the Method of Moments (MoM). Sample numerical results are presented and discussed for the current distribution as well as the input impedance and radiation pattern of the antenna. In particular, the EFIE solutions of the current distribution on an antenna in free space are checked with that obtained using a traditional approach of solving the Pocklington's equation. Also, the current distributions on an antenna above a very lossy half-space are checked by comparing them with that for the antenna above a PEC plane. Data of the current distribution and the input impedance show that for an antenna close to the media interface separating the two half-spaces, the electromagnetic parameters of the lower half-space can significantly affect the antenna characteristics. The radiation patterns of the antenna presented all exhibit properties as expected and similar to that documented in literature for infinitesimal vertical dipoles above a lossy half-space.

1. INTRODUCTION

Wire antennas are the oldest and perhaps still the most prevalent one of all antennas forms. For an accurate electromagnetic modeling of wire antennas, the electric current distributed on the wire must be determined [1]. In the past, Pocklington's equation [2] and Hallen's equations [3, 4] have been formulated by expressing the scattered electric field in terms of the magnetic vector potential and electric scalar potential, and then solved for the unknown current distribution on thin-wire antennas [1, 5]. This approach is widely used for analyzing wire antennas located in an *open* space where no media interface presents.

As pointed out in [6] and [7], the electromagnetic modeling of radiation by vertical dipole antennas above a lossy half-space has become an important subject of research and development, due to many applications where these antennas are involved. The modeling often encounters the Sommerfeld-type integrals [8] that represent the effect of the media interface. Asymptotic techniques, including the saddle-point method [9], have been developed to efficiently evaluate the Sommerfeld-type integrals. But these methods are limited for the evaluation of the Sommerfeld-type integrals involved in the far-zone field computations, which are not applicable for integral equation formulations that require information of the near-zone fields. In [7, 10], the input impedance of a vertical dipole antenna above a dielectric half-space is calculated, and an aperture antenna above a lossy half-space is analyzed, respectively. In the calculation and analysis, a complex image Green's function is used and a sinusoidal current distribution is assumed. However, the complex image Green's function is only an approximation of the exact Green's function, using a series of exponential functions, and the sinusoidal current assumption may not faithfully represent the actual current distribution, especially when the antenna is close to the media interface. Recently, an efficient computation of the electric field radiated by an infinitesimal electric dipole above a lossy half-space has been reported [11]. The efficient computation is based on an exact image theory [12–14] derived by means of applications of integral transforms and appropriate identities. In that way, the Sommerfeld-type integrals involved in the computation of the electric field are reduced to integrals that converge very rapidly, and the computation time is greatly reduced. Using such efficiently-computed electric field as the Green's function will make the application of an integral equation approach practical for determining the current distribution on the surface of a dipole antenna above a lossy half-space.

In this paper, an electric field integral equation (EFIE) is formulated for the current distribution on a vertical dipole antenna above a lossy half-space, where the Green's function is the vertical component of the electric field radiated by an infinitesimal vertical dipole, which is readily determined making use of the exact image theory and is presented in [11]. Then, the integral equation formulated is solved numerically employing the Method of Moments (MoM) [15]. The numerical solution of such formulated integral equation is expected to be more efficient because the semi-infinite integral included in the Green's function converges very rapidly. Finally, based on knowledge of the current distribution, the antenna characteristics of interest, such as the input impedance and the radiation pattern, are computed.

The outline of the rest of this paper is as follows. Section 2 presents the formulation of the EFIE for the unknown current distribution. In the formulation, we start with a vertical dipole antenna in free space, extend it to that for the antenna above a lossy half-space employing the exact image theory, and then incorporate them in the EFIE formulation. The numerical solution procedure of the EFIE, employing the MoM, is described in Section 3. Also in Section 3, sample numerical results of the current distribution on a vertical dipole antenna above a lossy half-space, as well as data of its input impedance and radiation pattern are presented and discussed. Finally, conclusions are drawn in Section 4.

2. FORMULATION OF THE ELECTRIC FIELD INTEGRAL EQUATION (EFIE)

As shown in Fig. 1, a vertical dipole antenna of length l and of a circular cross section with radius a is located above a planar interface $z = 0$ at a height h measured from the center of the vertical antenna. The interface separates two semi-infinite homogeneous spaces. The upper half-space ($z > 0$) is taken to be free space representing the air characterized by $(\mu_0, \varepsilon_0, \sigma = 0)$; and the lower half-space is assumed to be a lossy medium with electromagnetic parameters $(\mu_0, \varepsilon_r\varepsilon_0, \sigma \neq 0)$. The antenna has a very narrow feed gap at its center and is fed by a delta-gap source [5] so that the incident electric field can be expressed by $E_z^i = V\delta(z)$, where $\delta(z)$ is a delta function. Under the excitation, a z-directed electric current is induced on the surface of the antenna that can be viewed as a perfect electric conductor (PEC). To determine the unknown current distribution, an electric field integral equation (EFIE) is formulated in this section. Different from the Pocklington's equation and the Hallen's equation, the Green's function used in the integral equations formulation presented in this section is the electric

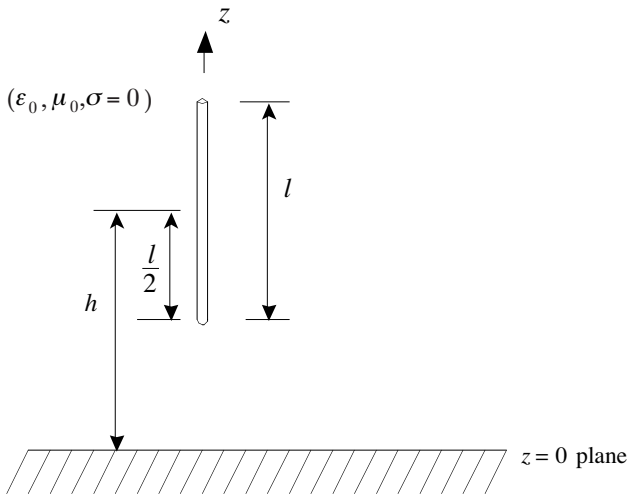

Figure 1. A vertical dipole antenna above a lossy half-space.

field, rather than the potentials, radiated by an infinitesimal vertical dipole above a lossy half-space. The EFIE is formulated by enforcing the boundary condition on a PEC surface, which requires that the tangential component of the total electric field be zero,

$$\vec{E}^s_{\tan} + \vec{E}^i_{\tan} = 0, \tag{1}$$

where $\vec{E}^s_{\tan}$ is the scattered electric field generated by the induced current and

$$\vec{E}^s_{\tan} = \vec{E}^f_{\tan} + E^d_{\tan}, \tag{2}$$

in which $\vec{E}^f_{\tan}$ is the electric field of the antenna if it were in free space and $\vec{E}^d_{\tan}$ is the diffracted field due to the existence of the lower half-space. Therefore, in this section, we present the electric field radiated by an infinitesimal vertical dipole in free space first, then derive the diffracted field by an infinitesimal vertical dipole above a lossy half-space, and finally, incorporate the electric fields in the EFIE formulation as the Green's function.

2.1. The Electric Field Radiated by an Infinitesimal Vertical Dipole in Free Space

The electric field radiated by an infinitesimal z-directed electric dipole of dipole moment Il in free space is given in [16], and its z-component

is readily found to be

$$E^f_{z,dipole} = Il\frac{e^{-jk_0R}}{4\pi R}jk_0\eta_0\left[\left(1-\frac{3j}{k_0R}-\frac{3}{k_0^2R^2}\right)\cos^2\theta-\left(1-\frac{j}{k_0R}-\frac{1}{k_0^2R^2}\right)\right], \tag{3}$$

where R is the distance between the source point and the field point, and $R = |\vec{r}-\vec{r}\,'| = \sqrt{(x-x')^2+(y-y')^2+(z-z')^2}$, in which (x', y', z') and (x, y, z) locate the source and field point, respectively. Also, in equation (3), k_0 and η_0 are the wavenumber and the intrinsic impedance of free space, and θ is the angle between vector $\vec{R}$ and the z-axis.

2.2. The Diffracted Electric Field of an Infinitesimal Vertical Dipole above a Lossy Half-space

The diffracted electric field of an infinitesimal dipole of orientation $\hat{l}$, where $\hat{l} = l_x\hat{x}+l_y\hat{y}+l_z\hat{z}$, located above a lossy half-space was originally derived by Sommerfeld and given in [11]

$$\begin{aligned}
\vec{E}^d_{dipole}(r,r') &= \hat{x}\frac{k_0\eta_0 I}{4\pi}\int_0^\infty\left\{\frac{k_\rho}{2k_z}\Gamma_h[-l_x(J_2(k_\rho\rho)\cos 2\phi + J_0(k_\rho\rho))\right.\\
&-l_yJ_2(k_\rho\rho)\sin 2\phi)] + \Gamma_v\frac{k_\rho}{2k_z}\left[\frac{2jk_zk_\rho}{k_0^2}l_z\cos\phi J_1(k_\rho\rho)\frac{k_z^2}{k_0^2}l_x(J_0(k_\rho\rho)\right.\\
&\left.\left.-J_2(k_\rho\rho)\cos 2\phi)-\frac{k_z^2}{k_0^2}l_yJ_2(k_\rho\rho)\sin 2\phi\right]\right\}e^{jk_z(z+z')}dk_\rho\\
&+\hat{y}\frac{k_0\eta_0 I}{4\pi}\int_0^\infty\left\{\Gamma_h\frac{k_\rho}{2k_z}[-l_xJ_2(k_\rho\rho)\sin 2\phi-l_y(J_0(k_\rho\rho)-J_2(k_\rho\rho)\cos 2\phi)]\right.\\
&+\Gamma_v\frac{k_\rho}{2k_z}\left[\frac{2jk_zk_\rho}{k_0^2}l_z\sin\phi J_1(k_\rho\rho) - \frac{k_z^2}{k_0^2}l_xJ_2(k_\rho\rho)\cos 2\phi\right.\\
&\left.\left.+\frac{k_z^2}{k_0^2}l_y(J_0(k_\rho\rho)+J_2(k_\rho\rho)\cos 2\phi)\right]\right\}e^{jk_z(z+z')}dk_\rho\\
&-\hat{z}\frac{k_0\eta_0 I}{4\pi}\int_0^\infty\frac{k_\rho}{k_z}\Gamma_v\left[\frac{k_\rho^2}{k_0^2}l_zJ_0(k_\rho\rho)+\frac{jk_zk_\rho}{k_0^2}J_1(k_\rho\rho)(l_x\cos\phi+l_y\sin\phi)\right]\\
&\times e^{jk_z(z+z')}dk_\rho,
\end{aligned} \tag{4}$$

where ρ is the radial distance between the observation and source points, ϕ is the angle between ρ and the x-axis, z and z' are the heights of the observation and source point above the lossy half-space, k_ρ and

k_z are spectral wave numbers and $k_z^2 = k_0^2 - k_\rho^2$. Also, in equation (4), $J_0(\cdot), J_1(\cdot)$, and $J_2(\cdot)$ are Bessel functions of order 0, 1 and 2, Γ_h and Γ_v are the horizontal and vertical Fresnel reflection coefficients given by

$$\Gamma_h = \frac{\eta_n - k_0/k_z}{\eta_n + k_0/k_z}, \qquad \Gamma_v = \frac{-\eta_n + k_z/k_0}{\eta_n + k_z/k_0} \tag{5a}$$

in which η_n is the normalized intrinsic impedance of the lower half-space, defined by

$$\eta_n = \eta/\eta_0 = \sqrt{1/[\varepsilon_r - j\sigma/(\omega\varepsilon_0)]}. \tag{5b}$$

For a vertical infinitesimal dipole, $l_x = 0,\ l_y = 0$, and $l_z = 1$, equation (4) reduces to

$$\vec{E}^d_{v,dipole}(r, r') = \frac{k_0\eta_0 Il}{4\pi}\int_0^\infty \frac{k_\rho}{k_z}\Gamma_v \left[\frac{jk_zk_\rho}{k_0^2}\cos\phi J_1(k_\rho\rho)\hat{x} + \frac{jk_zk_\rho}{k_0^2}\sin\phi J_1(k_\rho\rho)\hat{y} - \frac{k_\rho^2}{k_0^2}J_0(k_\rho\rho)\hat{z}\right] e^{jk_z(z+z')}dk_\rho. \tag{6}$$

One notes that the semi-infinite integral in (6) is a Sommerfeld-type integral, which does not have a closed-form analytic result, and is difficult to be evaluated numerically because of its poor convergence and highly oscillatory nature as shown in Fig. 2.

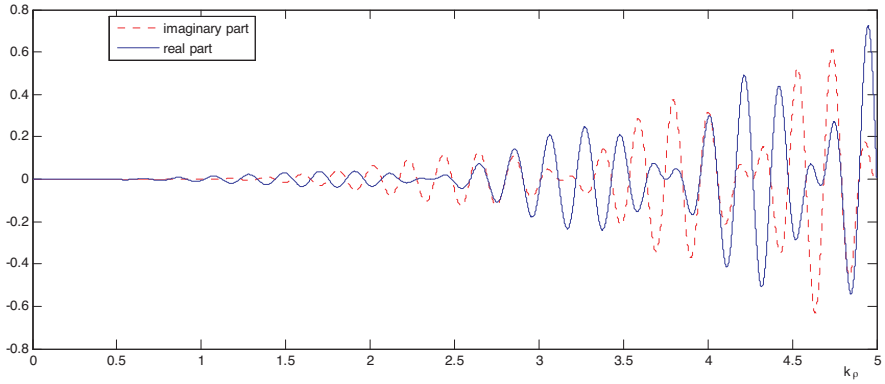

Figure 2. Highly oscillating integrand of the Sommerfeld-type integral $\int_0^\infty \frac{k_\rho^3}{k_z}\Gamma_v J_0(k_\rho\rho)e^{jk_z(z+z')}dk_\rho$ for $z+z' = 4,\ \rho = 30$ and $\eta_n = 0.3+j0.1$.

In order to improve the convergence property of the Sommerfeld-type integral, the exact image theory is employed by means of applications of integral transforms and appropriate identities as described in [11], the procedure is outlined below. First, equation (6) is rewritten to an equation that contains the zero-order Bessel function only as

$$\vec{E}^d_{v,dipole}(r,r') = -\frac{\eta_0 Il}{4\pi k_0}\left[\frac{\partial^2}{\partial x\partial z}\hat{x} + \frac{\partial^2}{\partial y\partial z}\hat{y} - \left(\frac{\partial^2}{\partial x^2} + \frac{\partial^2}{\partial y^2}\right)\hat{z}\right] \int_0^\infty \frac{k_\rho}{k_z}\Gamma_v J_0(k_\rho\rho)e^{jk_z(z+z')}dk_\rho, \tag{7}$$

by using the following identities

$$-j\cos\phi\frac{k_z k_\rho}{k_0^2}J_1(k_\rho\rho) = \frac{1}{k_0^2}\frac{\partial^2}{\partial x\partial z}J_0(k_\rho\rho), \tag{8a}$$

$$-j\sin\phi\frac{k_z k_\rho}{k_0^2}J_1(k_\rho\rho) = \frac{1}{k_0^2}\frac{\partial^2}{\partial y\partial z}J_0(k_\rho\rho), \tag{8b}$$

and

$$-\frac{k_\rho^2}{k_0^2}J_0(k_\rho\rho) = \frac{1}{k_0^2}\left(\frac{\partial^2}{\partial x^2} + \frac{\partial^2}{\partial y^2}\right)J_0(k_\rho\rho). \tag{8c}$$

Then, the vertical Fresnel reflection coefficient Γ_v contained in (7) is expressed in the form of a Laplace transform as

$$\Gamma_v = 1 - 2\eta_n k_0\int_0^\infty e^{-(\eta_n k_0 + k_z)\xi}d\xi. \tag{9}$$

Substituting equation (9) into (7) and then solving the resulting integrals in terms of k_ρ analytically by applying

$$\frac{e^{jkR''}}{R''} = j\int_0^\infty \frac{k_\rho}{k_z}J_0(k_\rho\rho)e^{jk_z(z+z')}dk_\rho, \tag{10}$$

where R'' is defined by $R'' = \sqrt{(x-x')^2 + (y-y')^2 + (z+z')^2}$, we arrive at the final form of $\vec{E}^d_{v,dipole}$ as

$$\vec{E}^d_{v,dipole}(\vec{r},\vec{r}') = -\frac{j\eta_0 Il}{4\pi k_0}\left[\frac{\partial^2}{\partial x\partial z}\hat{x} + \frac{\partial^2}{\partial y\partial z}\hat{y} - \left(\frac{\partial^2}{\partial x^2} + \frac{\partial^2}{\partial y^2}\right)\hat{z}\right] \left[\frac{e^{-jkR''}}{R''} - 2\eta_n k_0\int_0^\infty e^{-\eta_n k_0\xi}\frac{e^{-jk_0R'(\xi)}}{R'(\xi)}d\xi\right], \tag{11}$$

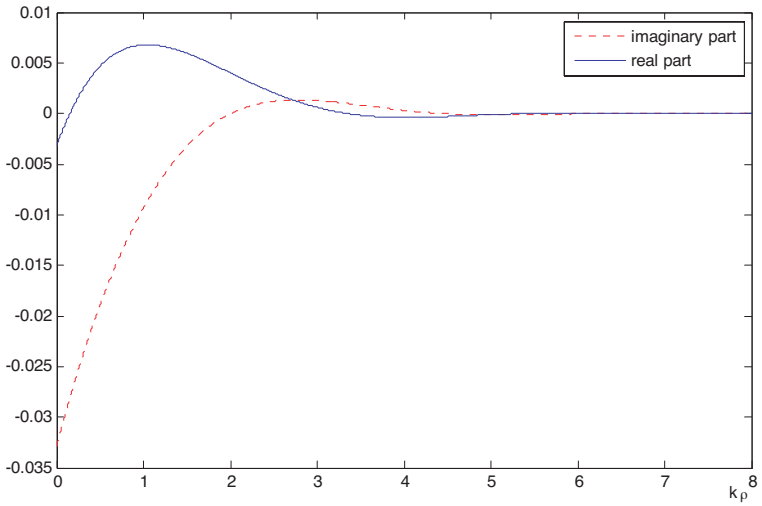

Figure 3. Rapidly decaying integrand of the semi-infinite integral $\int_0^\infty \frac{e^{-\eta_n k_0 \xi} e^{-jk_0 R'(\xi)}}{R'(\xi)} d\xi$ for $z + z' = 4,\ \rho = 30$ and $\eta_n = 0.3 + 0.1j$.

in which $R'(\xi)$ is defined by $R'(\xi) = \sqrt{(x-x')^2+(y-y')^2+(z+z'+j\xi)^2}$. As illustrated in Fig. 3, the integrand of the semi-infinite integral on the right-hand side of equation (11) with the same parameters as those used in Fig. 2 decays rapidly as ξ increases, due to both exponentially decaying factors $e^{-\eta_n k_0 \xi}$ and $e^{-jkR'(\xi)}$. Subsequently, the semi-infinite integral with such a rapidly decaying integrand will converge quickly, making the application of an integral equation approach practical, where $\vec{E}^d_{v,dipole}$ is to be used as part of the Green's function in the integral equation formulation.

2.3. Formulation of EFIE for a Vertical Dipole Antenna above a Lossy Half-space

Based on knowledge of the electric field of an infinitesimal dipole in free pace and the diffracted field by the dipole above a lossy half-space, derived in the previous two sub-sections, an EFIE is formulated for the current distributed on the surface of a vertical dipole antenna above a lossy half-space. The EFIE is formulated for a thin wire antenna, the radius of which is much less than the wavelength and the length of the antenna ($a \ll \lambda,\ a \ll l$). The current on the antenna surface is assumed to be in z direction and is independent of ϕ due to the azimuthal symmetry of the cylindrical configuration of the antenna,

and the current is supposed to vanish at the two ends of the antenna.

The first step of the formulation of the EFIE is to enforce the boundary condition which requires that the tangential component of the total electric field be zero on a PEC surface, as shown in equation (1). Under the assumption that the current distributed on the antenna surface is z-directed and ϕ-independent, the tangential component of the electric field should be E_z. Then, equation (1) reduces to

$$E_z^s + E_z^i = 0, \tag{12}$$

where E_z^i is the z-component of the incident electric field and

$$E_z^i = V\delta(z), \tag{13}$$

in which V is a voltage applied across a very narrow feed gap and $\delta(z)$ is a delta function. Also, in equation (12), E_z^i is the scattered field that contains the free-space-field term and the diffracted-field term as

$$E_z^s = E_z^f + E_z^d, \tag{14}$$

where E_z^f can be found as an integral, on the antenna surface, of the z-component of the electric field generated by an infinitesimal vertical dipole in free space, given in equation (3),

$$E_{z,dipole}^f = Il\frac{e^{-jk_0R}jk_0\eta_0}{4\pi R}\left[\left(1-\frac{3j}{k_0R}-\frac{3}{k_0^2R^2}\right)\left(\frac{z-z'}{R}\right)^2-\left(1-\frac{j}{k_0R}-\frac{1}{k_0^2R^2}\right)\right]. \tag{3'}$$

Also, in equation (14), the diffracted field E_z^d can be obtained as an integral, on the antenna surface, of the z-component of the diffracted field generated by an infinitesimal vertical dipole above the lossy half-space, given by equation (11) as

$$E_{z,dipole}^d = \frac{j\eta_0 Il}{4\pi k_0}\left(\frac{\partial^2}{\partial x^2}+\frac{\partial^2}{\partial y^2}\right)\left[\frac{e^{-jk_0R''}}{R''}-2\eta_n k_0\int_0^\infty e^{-\eta_n k_0\zeta}\frac{e^{-jk_0R'(\zeta)}}{R'(\xi)}d\xi\right]. \tag{11'}$$

Then, the total scattered field by the vertical dipole antenna can be found as the surface integral of $E_{z,dipole}^f$ and $E_{z,dipole}^d$, given in equations

(3') and (11'), and

$$E_z^s = \int_{z'=h-\frac{l}{2}}^{h+\frac{l}{2}} \int_{\phi'=-\pi}^{\pi} J_z a \left\{ \frac{jk_0\eta_0 e^{-jk_0R}}{4\pi R} \left[\left(1-\frac{3j}{k_0R}-\frac{3}{k_0^2R^2}\right)\left(\frac{z-z'}{R}\right)^2 - \left(1-\frac{j}{k_0R}-\frac{1}{k_0^2R^2}\right)\right] + \frac{j\eta_0}{4\pi k_0}\left(\frac{\partial^2}{\partial x^2}+\frac{\partial^2}{\partial y^2}\right) \times \left[\frac{e^{-jk_0R''}}{R''} - 2\eta_n k_0 \int_0^{\infty} e^{-\eta_n k_0 \zeta} \frac{e^{-jk_0R'(\zeta)}}{R'(\xi)} d\xi\right]\right\} dz' d\phi', \qquad (15)$$

in which J_z is the surface current density on the antenna surface. For convenience, we define a current as $I(z) = 2\pi a J_z(z)$. After substituting such defined $I(z)$ into (15) and taking the derivatives in the equation, we rewrite equation (15) as

$$E_z^s = \int_{z'=h-\frac{l}{2}}^{h+\frac{l}{2}} \frac{I(z')}{2\pi} \int_{\phi'=-\pi}^{\pi} \left\{ \frac{jk_0\eta_0 e^{-jk_0R}}{4\pi R} \left[\left(1-\frac{3j}{k_0R}-\frac{3}{k_0^2R^2}\right)\left(\frac{z-z'}{R}\right)^2 - \left(1-\frac{j}{k_0R}-\frac{1}{k_0^2R^2}\right)\right] + \frac{j\eta_0}{4\pi k_0} \times \frac{e^{-jk_0R''}\left[(3/R''+3jk_0-k_0^2R'')[(x-x')^2+(y-y')^2]-2R''(jk_0R''+1)\right]}{R''^4} - \frac{j\eta_0\eta_n}{2\pi}\int_0^{\infty} e^{-\eta_n k_0 \xi} \times \frac{e^{-jk_0R'}\left[(3/R'+3jk_0-k_0^2R')[(x-x')^2+(y-y')^2]-2R'(jk_0R'+1)\right]}{R'^4} d\xi \right\} \times dz' d\phi'. \qquad (16)$$

Finally, substituting equations (13) and (16) into (12), the EFIE is formulated as

$$\int_{z'=h-\frac{l}{2}}^{h+\frac{l}{2}} \frac{I(z')}{2\pi} \int_{\phi'=-\pi}^{\pi} \left\{ \frac{jk_0\eta_0 e^{-jk_0R}}{4\pi R} \left[\left(1-\frac{3j}{k_0R}-\frac{3}{k_0^2R^2}\right)\left(\frac{z-z'}{R}\right)^2 - \left(1-\frac{j}{k_0R}-\frac{1}{k_0^2R^2}\right)\right] + \frac{j\eta_0}{4\pi k_0} \times \frac{e^{-jk_0R''}\left[(3/R''+3jk_0-k_0^2R'')[(x-x')^2+(y-y')^2]-2R''(jk_0R''+1)\right]}{R''^4}$$

$$-\frac{j\eta_0\eta_n}{2\pi}\int_0^{\infty} e^{-\eta_n k_0\xi} \times\frac{e^{-jk_0R'}\left[(3/R'+3jk_0-k_0^2R')[(x-x')^2+(y-y')^2]-2R'(jk_0R'+1)\right]}{R'^4}d\xi\Bigg\} \times dz'd\phi' = -V\delta(z). \quad (17)$$

3. NUMERICAL SOLUTION TECHNIQUE, RESULTS, AND DISCUSSION

3.1. The Numerical Solution Technique

In this section, the EFIE formulated in the previous section is solved numerically, employing the MoM, for the unknown current $I(z)$ distributed on the surface of a vertical dipole antenna above a lossy half-space. Then, based on knowledge of the current distribution, the antenna characteristics of interest, such as the input impedance and the radiation pattern, are computed. Sample numerical results are presented and discussed.

One notes that the integral equation presented in equation (17) contains double integrals. To eliminate one of the double integrals for an efficient numerical solution of the integral equation, the reduced kernel approximation [5, 17] for thin wires [18–20] under the conditions that $a \ll \lambda$ and $a \ll l$ is employed. Realizing that for both the source point and field point on the antenna surface, the radial distance $d = (x-x')^2+(y-y')^2 = 4a^2\sin^2(\phi/2)$ can be approximated by its median value $d = a$ for a thin wire. Subsequently, R, R', and R'' in equation (17) can be approximated by $R \approx R_r = \sqrt{(z-z')^2+a^2}$, $R' \approx R'_r = \sqrt{a^2+(z+z'+j\xi)^2}$, and $R'' \approx R''_r = \sqrt{a^2+(z+z')^2}$; then the integrands in the integrals of (17) become ϕ-independent. Thus, the integral equation reduces to

$$\int_{z'=h-\frac{l}{2}}^{h+\frac{l}{2}} I(z)\left\{\frac{jk_0\eta_0e^{-jk_0R_r}}{4\pi R_r}\left[\left(1-\frac{3j}{k_0R_r}-\frac{3}{k_0^2R_r^2}\right)\left(\frac{z-z'}{R_r}\right)^2 - \left(1-\frac{j}{k_0R_r}-\frac{1}{k_0^2R_r^2}\right)\right]+\frac{j\eta_0}{4\pi k_0} \times\frac{e^{-jk_0R''_r}\left[(3/R''_r+3jk_0-k_0^2R''_r)\cdot a^2-2R''_r(jk_0R''_r+1)\right]}{R''^4_r} -\frac{j\eta_0\eta_n}{2\pi}\int_0^{\infty} e^{-\eta_n k_0\xi}$$

$$\times \frac{e^{-jk_0R'_r}\left[(3/R'_r + 3jk_0 - k_0^2R'_r)\cdot a^2 - 2R'_r(jk_0R'_r+1)\right]}{{R'_r}^4} d\xi \Bigg\} dz'd\phi'$$
$$= -V\delta(z). \tag{18}$$

To solve the integral equation (18), the MoM is employed. First, we divide the vertical antenna into N segments, the length of each is $\Delta = l/N$, then express the unknown current $I(z)$ as a linear combination of pulse function

$$I(z) = \sum_{n=1}^{N} I_n \Pi_n(z), \tag{19}$$

where the pulse function is defined by

$$\Pi_n(z) = \begin{cases} 1, & z \in (z_n - \dfrac{\Delta}{2}, z_n + \dfrac{\Delta}{2}) \\ 0, & \text{otherwise} \end{cases} \tag{20}$$

in which z_n is the median point of the nth segment. Then, substituting the pulse expansion for $I(z)$ in (18) and then testing the resulting equation with the pulse function; the integral equation is converted to a matrix equation as

$$[Z_{mn}][I_n] = [V_m], \tag{21}$$

where the forcing function is

$$V_m = \int_{h-\frac{l}{2}}^{h+\frac{l}{2}} E_z^i(z)\Pi_m(z)dz \tag{22}$$

and the impedance matrix elements Z_{mn} are given by

$$\begin{aligned} Z_{mn} \;=\; & \int_{z=-\frac{\Delta}{2}}^{\frac{\Delta}{2}} \int_{z'=-\frac{\Delta}{2}}^{\frac{\Delta}{2}} \left\{ \frac{jk_0\eta_0 e^{-jk_0R_r}}{4\pi R_r} \left[\left(1 - \frac{3j}{k_0R_r} - \frac{3}{k_0^2R_r^2}\right) \right.\right. \\ & \left.\left. \left(\frac{(m-n)\Delta - z'}{R_r}\right)^2 - \left(1 - \frac{j}{k_0R_r} - \frac{1}{k_0^2R_r^2}\right)\right] + \frac{j\eta_0}{4\pi k_0} \right. \\ & \left. \times \frac{e^{-jk_0R''_r}\left[(3/R''_r + 3jk_0 - k_0^2R''_r)\cdot a^2 - 2R''_r(jk_0R''_r+1)\right]}{{R''_r}^4} \right. \\ & \left. - \frac{j\eta_0\eta_n}{2\pi} \int_0^{\infty} e^{-\eta_n k_0 \xi} \right. \end{aligned}$$

$$\times \frac{e^{-jk_0R'_r}\left[(3/R'_r + 3jk_0 - k_0^2R'_r)\cdot a^2 - 2R'_r(jk_0R'_r+1)\right]}{{R'_r}^4} d\xi \Bigg\} dz'dz, \tag{23}$$

in which,

$$R_r = \sqrt{a^2+((m-n)\Delta - z')^2}, \quad R''_r = \sqrt{(2h-l+(m+n)\Delta+z')^2+a^2},$$

and

$$R'_r = \sqrt{(2h-l+(m+n)\Delta+z'-j\xi)^2+a^2}.$$

Based on knowledge of the current distribution on the surface of a center-fed antenna, its input impedance can be readily found by

$$Z_{in} = V/I(h), \tag{24}$$

where V is taken to be 1 volt and $I(h)$ is the input current at the feeding point $z = h$. Also, the far-zone radiation pattern of the antenna can be found [21] by

$$F_u(\theta) = \sin\theta \int_{h-\frac{l}{2}}^{h+\frac{l}{2}} I(z')(e^{jk_0z'\cos\theta} + \Gamma e^{-jk_0z'\cos\theta})dz' \quad -\pi/2 < \theta < \pi/2, \tag{25}$$

where

$$\Gamma = \frac{\cos\theta/\eta_n^2 - \sqrt{1/\eta_n^2 - \sin^2\theta}}{\cos\theta/\eta_n^2 + \sqrt{1/\eta_n^2 - \sin^2\theta}}, \tag{26}$$

for the upper half-space. And

$$F_l(\theta) = \sin\theta e^{-jkR} \int_{h-\frac{l}{2}}^{h+\frac{l}{2}} I(z')Te^{jkz'\cos\theta}dz' \quad \pi/2 < \theta < 3\pi/2, \tag{27}$$

where

$$T = \frac{2\cos\theta}{\eta_n\cos\theta - \sqrt{1-\sin^2\theta/\eta_n^2}}, \tag{28}$$

for the lower half-space. In equations (25) and (27), k_0 and k are the wavenumbers in the upper and lower half-space, respectively.

3.2. Numerical Results and Discussion

Sample numerical results of the current $I(z)$ distributed on the surface of a thin-wire vertical antenna above a lossy half-space as well as the input impedance and radiation pattern of the antenna are presented and discussed in this section. First of all, the EFIE results of the current distribution on a half-wavelength-long thin-wire antenna ($a = 0.01\lambda$) located in free-space are checked by comparing them with that obtained by a traditional approach of solving the Pocklington's equation. The comparison is illustrated in Fig. 4, where one observes that the two sets of data resulting from these two methods fall on top of each other. The same comparison is also made for a one-wavelength-long thin-wire antenna in free-space, and is presented in Fig. 5, which shows again that the EFIE results are almost the same as the Pocklington's equation solutions, as they should be.

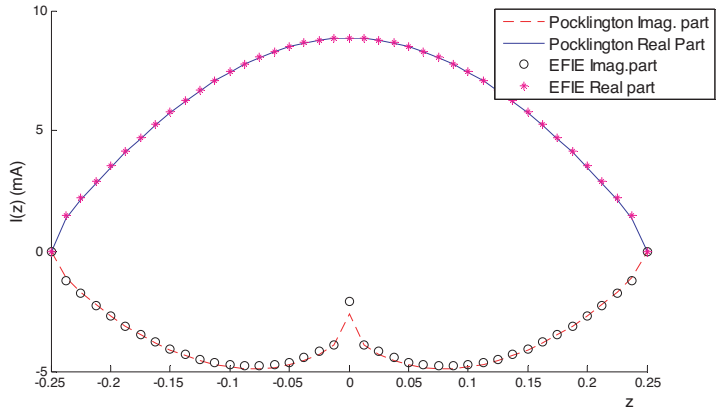

Figure 4. Comparison between the current distributions obtained using Pocklington's eq. and that employing EFIE on a thin-wire vertical antenna ($a = 0.01\lambda,\ l = 0.5\lambda$) in free space.

Then, data of the current distribution on a half-wavelength-long thin-wire antenna ($a = 0.01\lambda$) above a lossy half-space of various conductivities are checked by comparing them with that on the antenna above a PEC plane. The comparisons are illustrated in Fig. 6 for $h = 0.26\lambda$ and Fig. 7 for $h = 0.35\lambda$. From these two figures, one observes that as the conductivity of the lower half-space increases, the current distribution gradually approaches to that for the antenna above a PEC plane. When the conductivity is taken to be high enough ($\sigma = 10^4$), the two sets of data match very well, as one would expect.

Fig. 8 depicts data of the current distributed on the surface of a

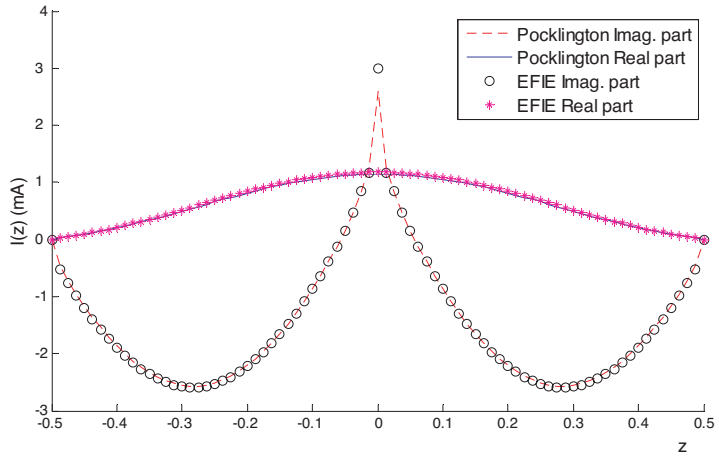

Figure 5. Comparison between the current distributions obtained using Pocklington's eq. and that employing EFIE on a thin-wire vertical antenna ($a = 0.01\lambda,\ l = 1\lambda$) in free space.

thin-wire antenna ($a = 0.01\lambda,\ l = 0.5\lambda$) above a lossy half-space with normalized intrinsic impedance $\eta_n = 0.3 + j0.1$, at different heights. One notes from the data that when the antenna is very close to the media interface separating the two half-spaces ($h = 0.26\lambda$), its current distribution is significantly different from that obtained for the antenna located in free space. However, as the height of the antenna increases, the current distribution data gradually approach to the free-space result. This makes sense because when the antenna location is moved away from the media interface, the influence of the lower half-space on the antenna current distribution becomes weaker and weaker. If the antenna is located high enough above the lossy half-space, then the influence of the lower half-space on the antenna would be negligible, making its current distribution be about the same as the free-space results.

To see how the electromagnetic parameters of the lower half-space can affect the current distribution on an antenna above it, in Figs. 9 and 10, we present the current distribution on a thin-wire vertical antenna ($a = 0.01\lambda,\ l = 0.5\lambda$) above the lower half-space, at a height of $h = 0.251\lambda$, with various normalized intrinsic impedance η_n. In Fig. 9, the imaginary part of η_n is taken to be unchanged, only its real part varies. The data presented in Fig. 10 are for the case that the real part of η_n remains to be a fixed value, only its imaginary part changes. The data depicted in these two figures show that when

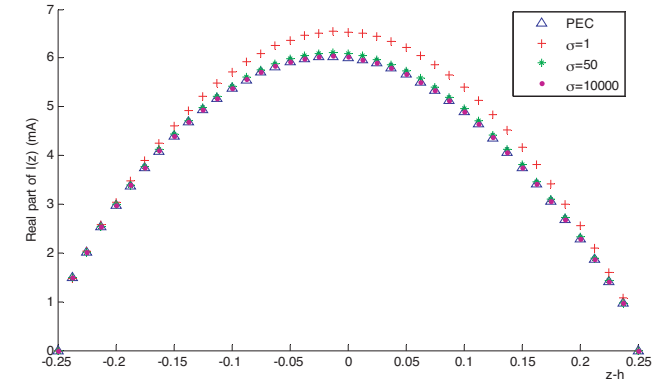

(a) Real part

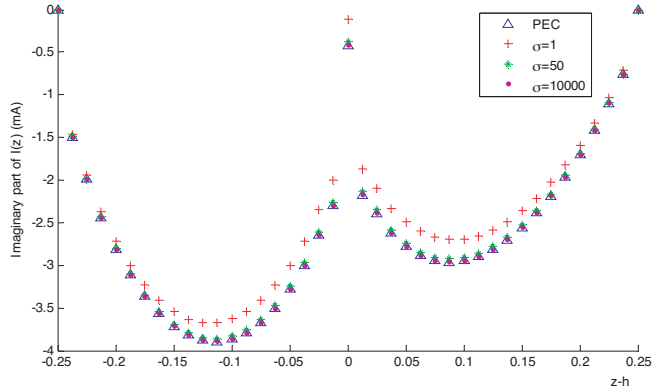

(b) Imaginary part

Figure 6. Comparison between the current distributions on a vertical dipole antenna ($a = 0.01\lambda$, $l = 0.5\lambda$) above a lossy half-space ($\varepsilon_r = 1.001$, $h = 0.26\lambda$, $f = 300\,\text{MHz}$) of various conductivities with that on the antenna above a PEC plane.

the normalized intrinsic impedance of the lower half-space varies, the current distribution changes, and they all are significantly different from that for the antenna located in free space.

Based on knowledge of the current distribution on a thin-wire antenna above a lossy half-space, its input impedance and radiation pattern are obtained and presented in Tables 1–3 and Figs. 11–12, all for $a = 0.01\lambda$ and $l = 0.5\lambda$. In Table 1 are listed data of the input impedance $\eta_n = 0.3 + j0.1$of the antenna above a lossy half-space with

Table 1. The input impedance of a vertical dipole antenna ($a = 0.01\lambda,\ l = 0.5\lambda$) above a lossy half-space ($\eta_n = 0.3+0.1j$) with various heights.

	$Z_{in}(\Omega)$
Free space result	$106.8188 + 25.1592j$
$h = 2\lambda$	$106.7627 + 25.2726j$
$h = 1\lambda$	$107.3416 + 24.2268j$
$h = 0.5\lambda$	$103.0509 + 18.2636j$
$h = 0.26\lambda$	$132.4766 + 6.4395j$

Table 2. The input impedance of a vertical dipole antenna ($a = 0.01\lambda,\ l = 0.5\lambda,\ h = 0.251\lambda$) above a half-space with various real part of normalized intrinsic impedance.

	$Z_{in}(\Omega)$
Free space result	$106.8188 + 25.1592j$
$\eta_n = 0.05 + 0.1j$	$198.8489 - 9.8498j$
$\eta_n = 0.12 + 0.1j$	$183.6976 - 4.7526j$
$\eta_n = 0.2 + 0.1j$	$168.5355 - 0.4902j$
$\eta_n = 0.3 + 0.1j$	$152.2572 + 3.2005j$

Table 3. The input impedance of a vertical dipole antenna ($a = 0.01\lambda,\ l = 0.5\lambda,\ h = 0.251\lambda$) above a half-space with various imaginary part of normalized intrinsic impedance.

	$Z_{in}(\Omega)$
Free space result	$106.8188 + 25.1592j$
$\eta_n = 0.3 + 0.01j$	$153.9227 + 17.1085j$
$\eta_n = 0.3 + 0.1j$	$152.2572 + 3.2005j$
$\eta_n = 0.3 + 0.15j$	$150.474 - 4.1298j$
$\eta_n = 0.3 + 0.23j$	$146.5436 - 15.0825j$

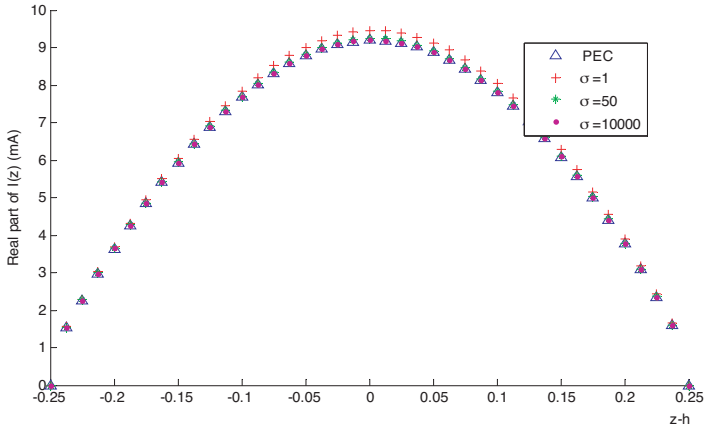

(a) Real part

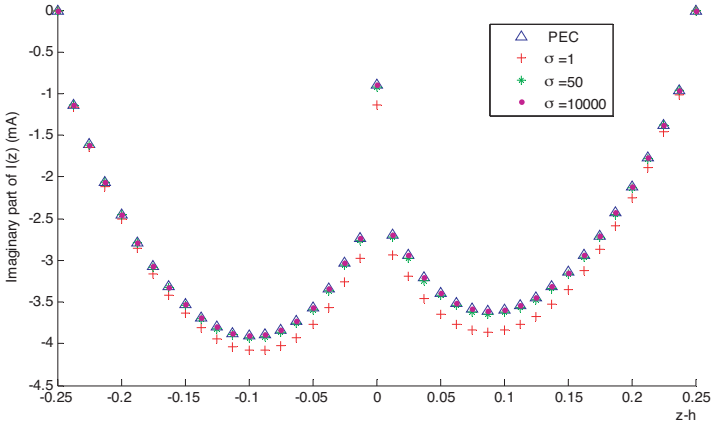

(b) Imaginary part

Figure 7. Comparison between the current distributions on a vertical dipole antenna ($a = 0.01\lambda$, $l = 0.5\lambda$) above a lossy half-space ($\varepsilon_r = 1.001$, $h = 0.35\lambda$, $f = 300\,\mathrm{MHz}$) of various conductivities with that on the antenna above a PEC plane.

normalized intrinsic impedance, at different heights. One observes that when the antenna is very close to the media interface separating the two half-spaces, its input impedance is significantly different from that for the antenna located in free space. As the height of the antenna increases, its input impedance gradually approaches to the free-space

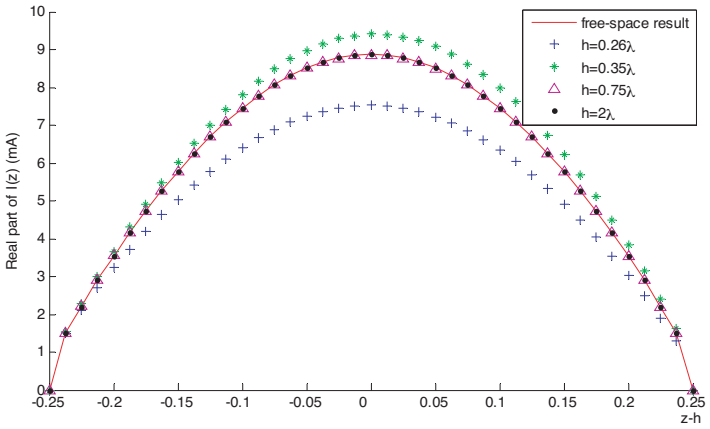

(a) Real part

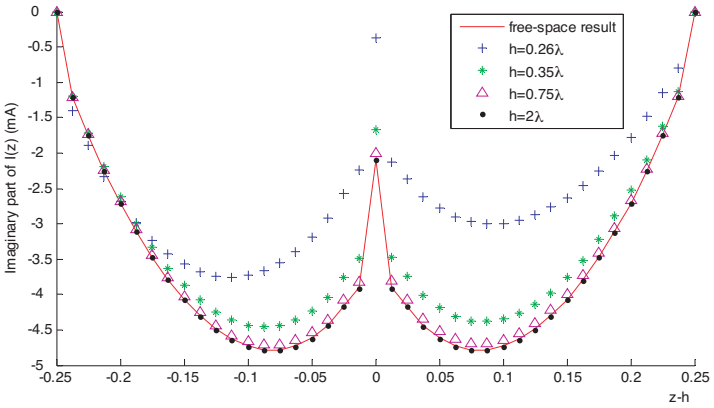

(b) Imaginary part

Figure 8. Current distributions on a vertical dipole antenna ($a = 0.01\lambda$, $l = 0.5\lambda$) at different heights above a half-space with normalized intrinsic impedance $\eta_n = 0.3 + j0.1$.

result. Again, this is what one would expect and is due to the fact that as the antenna is placed farther and farther apart from the media interface, the influence of the lower half-space becomes weaker and weaker, and eventually negligible if the antenna is located high enough above the interface. Tables 2 and 3 present the input impedance for the antenna above a lossy half-space, at a height of $h = 0.251\lambda$, with different normalized intrinsic impedance η_n. Data listed in these two tables show that variation of the electromagnetic parameters of the

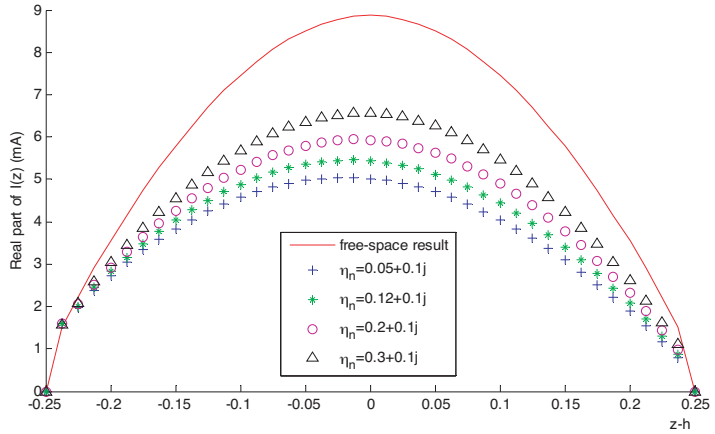

(a) Real part

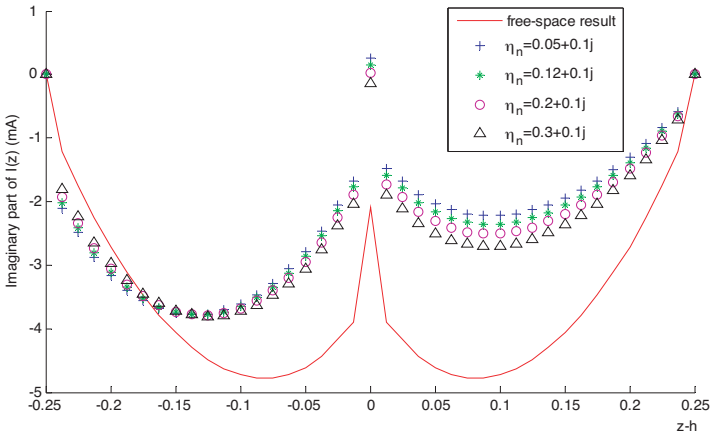

(b) Imaginary part

Figure 9. Current distributions on a vertical dipole antenna ($a = 0.01\lambda,\ l = 0.5\lambda,\ h = 0.251\lambda$) above a half-space with various real part of normalized intrinsic impedance.

lower half-space can significantly change the input impedance of a vertical antenna above it.

Radiation patterns of an antenna above a lossy half-space are presented in Figs. 11 and 12. Fig. 11 depicts the radiation patterns of an antenna above a very lossy half-space. One observes that as the conductivity increases, the magnitude of the field in the upper half-space becomes larger and larger, and the radiation patterns gradually

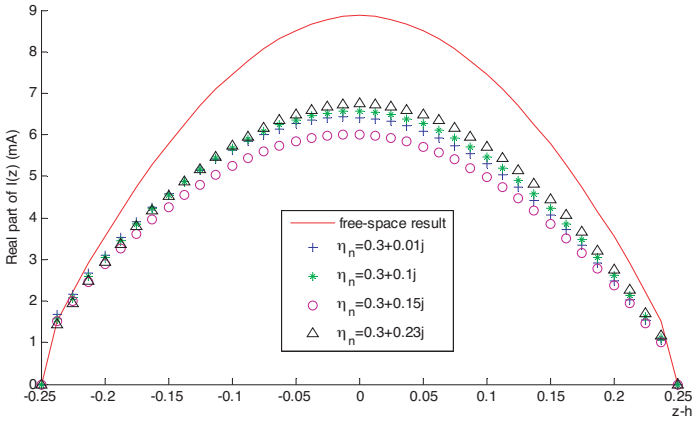

(a) Real part

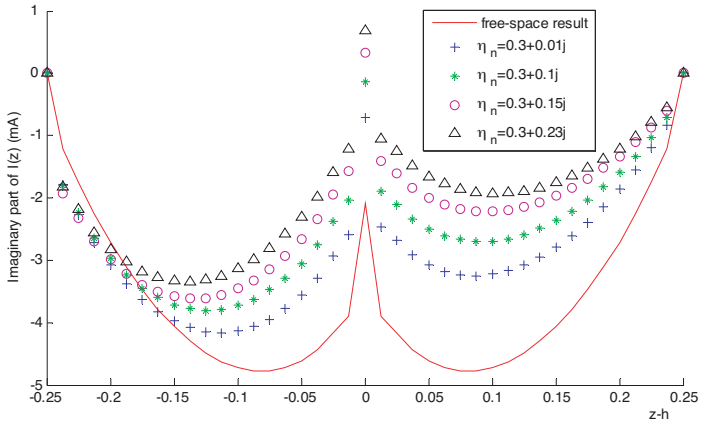

(b) Imaginary part

Figure 10. Current distributions on a vertical dipole antenna ($a = 0.01\lambda$, $l = 0.5\lambda$, $h = 0.251\lambda$) above a half-space with various imaginary part of normalized intrinsic impedance.

approach to that for the antenna above a PEC plane. This is expected and is similar to that presented in [21] for an infinitesimal vertical dipole above a very lossy half-space. Fig. 12 presents the radiation patterns corresponding to different antenna heights. One notes that for an antenna with larger height h above the lower half-space, its radiation pattern has more lobes. This phenomenon is similar to that presented

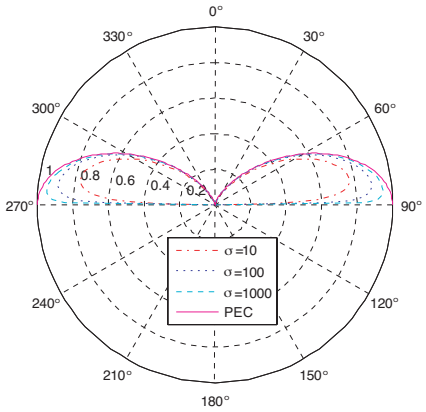

Figure 11. Radiation patterns of a vertical dipole antenna ($a = 0.01\lambda$, $l = 0.5\lambda$) above a very lossy half-space ($\varepsilon_r = 1.001$, $h = 0.26\lambda$, $f = 300\,\text{MHz}$) of various conductivities, compared with that for the antenna above a PEC plane.

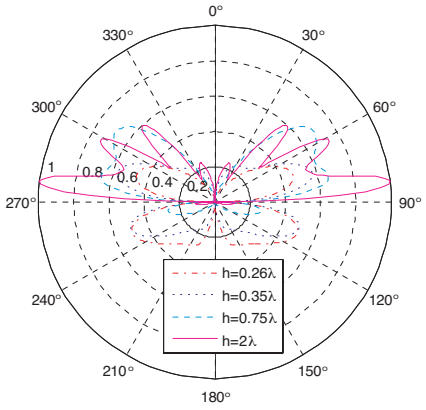

Figure 12. Radiation patterns of a vertical dipole antenna ($a = 0.01\lambda$, $l = 0.5\lambda$) at different heights above a lossy half-space with normalized intrinsic impedance $\eta_n = 0.3 + j0.1$.

and discussed in [21] and [22] for infinitesimal vertical dipoles above a lossy half-space. The magnitude of the far-zone field in the lossy lower half-space is supposed to be very small, due to an exponentially decaying factor e^{-jkR} in equation (29). In order to provide information of the angular distribution of the field in the lower half-space, the field pattern depicted for that region is enlarged by a factor of $1/e^{-jkR}$.

4. CONCLUSIONS

In this paper, an EFIE is formulated and solved numerically for an efficient analysis of a vertical thin-wire antenna above a lossy half-space. In the EFIE formulation, the Sommerfeld-type integrals, which are often encountered in electromagnetic modeling involving media interfaces, are reduced to semi-infinite integrals that converge rapidly making use of the exact image theory. The EFIE solutions of the current distribution on an antenna in free space have been checked with that obtained using a traditional approach of solving the Pocklington's equation, and a good agreement is observed. A comparison between the current distributions on an antenna above a lossy half-space of various conductivities with that on the antenna above a PEC plane illustrates that as the conductivity increases, the current distribution data gradually approach to that for the antenna above a PEC plane. And when the conductivity is taken to be high enough, the two sets of data match each other, as one would expect. Data of the current distributed on an antenna above a lossy half-space at different heights show that for an antenna close to the media interface separating the two half-spaces, the lower half-space can significantly affect the current distribution on the antenna and its input impedance. But as the antenna is located farther apart from the lower half-space, its influence would become weaker and weaker, and eventually negligible if the antenna is placed high enough above the lower half-space. The radiation patterns of an antenna above a lossy half-space of various conductivities show that the magnitude of the field in the upper half-space becomes larger and larger and the radiation patterns approach to that for the antenna above a PEC plane, as the lower half-space conductivity increases. The radiation patterns for an antenna above a lossy half-space at different heights illustrate that as the height increases; the field pattern in the upper half-space has more lobes. All these properties of the radiation patterns presented are similar to that documented in literature for infinitesimal dipoles above a lossy half-space.

REFERENCES

1. Elliott, R. S., *Antenna Theory and Design*, Prentice-Hall Inc., Englewood Cliffs, New Jersey 07632, 1981.
2. Pocklington, H. C., "Electrical oscillations in wire," *Cambridge Phil. Soc. Proc.*, Vol. 9, 324–332, 1897.
3. Hallen, E., "Theoretical investigations into transmitting and

receiving qualities of antennas," *Nova Acta Regiae Soc. Sci. Upsaliensis*, 1–44, January 1938.

4. Saadatmandi, A., M. Bazzaghi, and M. Dehghan, "Sinc-collocation methods for the solution of Hallen's integral equation," *Journal of Electromagnetic Waves and Applications*, Vol. 19, No. 2, 245–256, 2005.
5. Butler, C. M., "Integral equation method," ECE 839 Lecture Notes, Clemson University, Clemson, SC 29634-0915.
6. Wait, J. R., *Electromagnetic Waves in Stratified Media*, Pergamon, New York, 1970.
7. Shubair, R. M. and Y. L. Chow, "A closed-form solution of vertical dipole antennas above a dielectric half-space," *IEEE Transactions on Antennas and Propagation*, Vol. 41, No. 12, 1737–1741, December 1993.
8. Sommerfeld, A., *Partial Differential Equations*, Academic Press, New York, 1949.
9. Felson, L. B. and N. Marcuvitz, *Radiation and Scattering of Waves*, Prentice Hall Inc., Englewood Cliffs, New Jersey, 1973.
10. Arand, B. A., et al., "Analysis of aperture antennas above lossy half-space," *Progress In Electromagnetics Research*, PIER 44, 39–55, 2004.
11. Sarabandi, K., M. D. Casciato, and I.-S. Koh, "Efficient Calculation of the fields of a dipole radiating above an impedance surface," *IEEE Transactions on Antennas and Propagation*, Vol. 50, No. 9, 1222–1235, September 2002.
12. Lindell, I. V. and E. Alanen, "Exact image theory for Sommerfeld half-space problems, Part I: Vertical magnetic dipole," *IEEE Transactions on Antennas and Propagation*, Vol. AP-32, No. 2, 126–133, February 1984.
13. Lindell, I. V. and E. Alanen, "Exact image theory for Sommerfeld half-space problems, Part II: Vertical electric dipole," *IEEE Transactions on Antennas and Propagation*, Vol. AP-32, No. 10, 1027–1032, October 1984.
14. Lindell, I. V. and E. Alanen, "Exact image theory for Sommerfeld half-space problems, Part III: Vertical electric dipole," *IEEE Transactions on Antennas and Propagation*, Vol. AP-32, No. 8, 841–847, August 1984.
15. Harrington, R. F., *Field Computation by Moment Methods*, Robert E. Krieger Publishing Company, Malabar, Florida, 1982.
16. Harrington, R. F., *Time-Harmonic Electromagnetic Fields*, IEEE Press, John Wiley and Sons, Inc., 2001.

17. King, R. W. P., *The Theory of Line Antennas*, Harvard University, Cambridge, MA, 1956.
18. Papakanellos, P. J. and G. Fikioris, "A possible remedy for the oscillations occurring in thin-wire mom analysis of cylindrical antennas," *Progress In Electromagnetics Research*, PIER 69, 77–92, 2007.
19. Sijher, T. S. and A. A. Kishk, "Antenna modeling by infinitesimal dipoles using genetic algorithms," *Progress In Electromagnetics Research*, PIER 52, 225–254, 2005.
20. Zhang, X. J. et al., "Near field and surface field analysis of thin wire antenna in the presence of conducting tube," *Progress In Electromagnetics Research*, PIER 45, 313–333, 2004.
21. Stutzman, W. L., *Antenna Theory and Design*, John Wiley and Sons, Inc., 1981.
22. Balanis, C. A., *Antenna Theory Analysis and Design*, John Willy & Sons, Inc., 1997.